



HAL
open science

Bioinspired Nanotubes by Soft-template Electropolymerization from Fully Conjugated Monomers

Pape Diene Dione, Abdoulaye Dramé, Alioune Diouf, Frédéric Guittard,
Thierry Darmanin

► **To cite this version:**

Pape Diene Dione, Abdoulaye Dramé, Alioune Diouf, Frédéric Guittard, Thierry Darmanin. Bioinspired Nanotubes by Soft-template Electropolymerization from Fully Conjugated Monomers. *ChemistrySelect*, 2023, 8 (44), pp.e202300908. 10.1002/slct.202300908 . hal-04299985

HAL Id: hal-04299985

<https://hal.science/hal-04299985>

Submitted on 22 Nov 2023

HAL is a multi-disciplinary open access archive for the deposit and dissemination of scientific research documents, whether they are published or not. The documents may come from teaching and research institutions in France or abroad, or from public or private research centers.

L'archive ouverte pluridisciplinaire **HAL**, est destinée au dépôt et à la diffusion de documents scientifiques de niveau recherche, publiés ou non, émanant des établissements d'enseignement et de recherche français ou étrangers, des laboratoires publics ou privés.

Bioinspired Nanotubes by Soft-template Electropolymerization from Fully Conjugated Monomers

Pape Diene Dione,^[a] Abdoulaye Dramé,^[a] Alioune Diouf,^[a] Frédéric Guittard,^[b] and Thierry Darmanin^{[b]}*

^[a] P. D. Dione, Dr. A. Dramé, Prof. A. Diouf

Université Cheikh Anta Diop, Faculté des Sciences et Techniques, Département de Chimie,
B.P. 5005 Dakar, Sénégal.

^[b] Prof. F. Guittard, Dr. T. Darmanin

Université Côte d'Azur, NICE Lab, 06100 Nice, France.

E-mail: thierry.darmanin@univ-cotedazur.fr

<https://univ-cotedazur.fr/laboratoires/nature-inspires-creativity-engineers-n-i-c-e-lab>

Bioinspired by the strong water-adhesive forces of gecko foot or rose petals, here, nanotubular structures are prepared by soft-template electropolymerization. Water is mixed to a solvent of low water-solubility to form a micellar solution in the presence of tetrabutylammonium perchlorate as the electrolyte and surfactant. As the monomer, a benzene is trifunctionalized with various thiophene and carbazole moieties. The monomers are fully conjugated to favor the deposition compared to polymerization, as confirmed by cyclic voltammetry experiments. The surface nanostructures (nanotubes, nano-ribbons, coral-like structures) are highly dependent on the monomer and the water content but less on the deposition method. The maximum water contact angle is 158.1° accompanied with strong water adhesive force. These surfaces are highly interesting for applications in water-harvesting systems or in sensing platforms.

Introduction

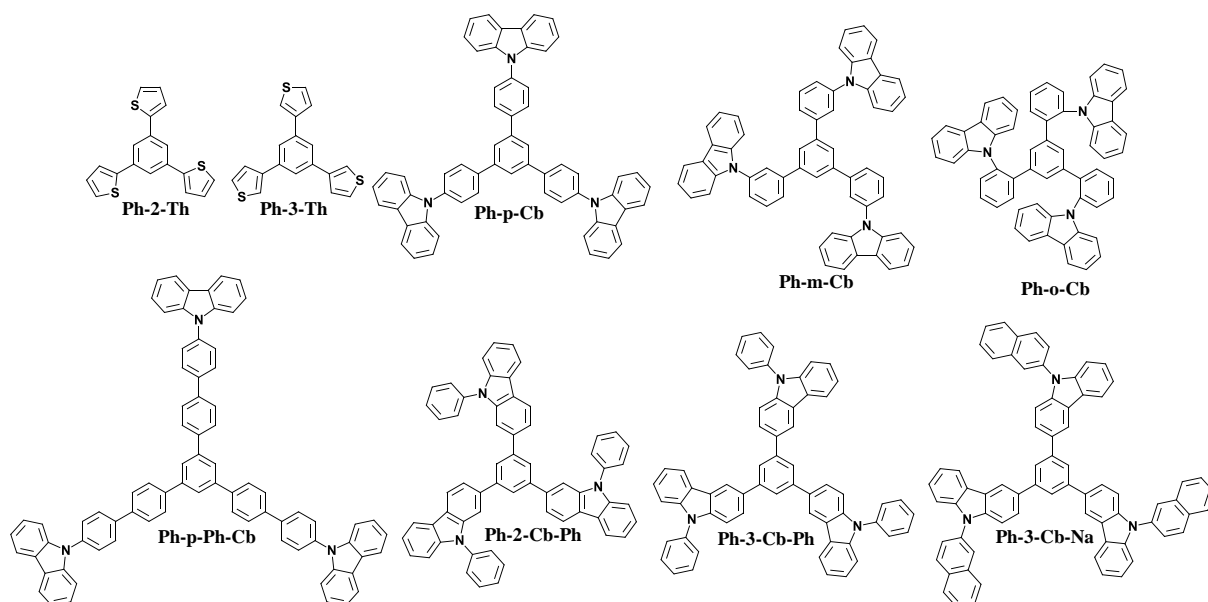
The control of structures at the nanoscale is fundamental in various practical applications including the areas of optical technologies, electronics, structural materials, catalysts, energy/environment, information technology, detection science, medicine^[1-4] but also for applications based on wetting properties.^[5-8] In Nature, there are many species having very

different liquid-repellencies. The most famous example is the lotus leaf with superhydrophobic and self-cleaning properties along with extremely both high water contact angles and ultra-low adhesion water and dust.^[9] By contrast, other species have ultra-strong water adhesion such as gecko foot or rose petal.^[10–13] These last properties could be used in water-harvesting systems or in sensing platforms.^[14,15] The key parameters for the control of liquid-repellency are the surface energy and the surface structures.^[16,17]

As surface structures, nanotubes are excellent candidates for their high surface-area-to-volume ratio, and also as demonstrated by Jiang et al. by comparing the water adhesive force between nanotubes and surfaces structures without nanopores. The work is fundamental because they prepared aligned polystyrene (PS) nanopillars terminating in flat, concave tips or nanotubes and the obtained surfaces display both the contact angles larger than 150° (superhydrophobicity) but the water adhesion was highly dependent on the tip geometry.^[18] Moreover, these forces are also highly dependent on the geometrical parameters of the tubes and the number of tubes.^[18–20] One of the most used methods for elaborating well-defined nanotubes on a substrate consists in the use of pre-formed hard templates such as anodized aluminum oxide (AAO) membranes.^[21,22] However, this method is very hard to implement and especially one novel membrane is necessary for each change in the nanotube geometrical parameters.

In soft-template electropolymerization or templateless electropolymerization, soft matter such as gas bubbles or micelles in solution can play a similar work than templates but there are extremely easy to form and remove.^[23–29] If the monomer is soluble in water (H₂O) such as pyrrole or aniline, gas bubbles can be produced *in-situ* if the electropolymerization is made in H₂O due to H₂O oxidation and/or reduction.^[23–26] If the monomer is insoluble in H₂O, the electropolymerization can be made in solvent of low water-solubility such as dichloromethane (CH₂Cl₂) or chloroform (CHCl₃).^[27–29] If H₂O is present in CH₂Cl₂ or chloroform CHCl₃, inverse micelles can be formed in solution acting as soft-template.^[27] For forming nanofibers by electropolymerization or nanotubes by soft-template electropolymerization, it is necessary to induce a preferential growth in one direction.^[30] It is well established in conjugated polymers that π -stacking interactions can induce this effect in the direction perpendicular to the molecule, as already reported with 3,4-naphthalenedioxythiophene (NaphDOT).^[27] Because the preferential growth needs time, the polymerization speed should not be too fast also, as already reported by designing monomers leading to only dimers during electropolymerization or by reducing the electropolymerization temperature.^[31,32] Wang et al. reported 1,3,5-tri(thiophen-2-yl)benzene (**Ph-2-Th**) as an excellent monomer by soft-template

electropolymerization in similar conditions.^[33] Here (Scheme 1), we study also a close monomer differing by the position of the thiophene groups (**Ph-3-Th**) as well as various original carbazole-based monomers (**Ph-p-Cb**, **Ph-m-Cb**, **Ph-o-Cb**, **Ph-p-Ph-Cb**, **Ph-2-Cb-Ph**, **Ph-3-Cb-Ph**, **Ph-3-Cb-Na**). All these monomers are fully conjugated in order to facilitate the deposition compared to polymerization. We want to show and explain how even just the position of a substituent can highly modify the resulting surface structures by soft-template electropolymerization. Particularly, we characterize the composition of the electrodeposits by electrochemical methods to show the presence of both monomers and oligomers in the films.



Scheme 1. Investigated monomers based on 1,3,5-triphenyl common core.

Results and Discussion

Soft-Template Electropolymerization

The monomer synthesis and the electrochemical parameters are available in Supporting Information. In order to investigate the effect of H₂O in soft-template electropolymerization, two solvents were studied here: dichloromethane (CH₂Cl₂) and dichloromethane saturated with water (CH₂Cl₂ + H₂O sat.). Tetrabutylammonium perchlorate (Bu₄NClO₄) was used as supporting electrolyte and also for stabilizing the micelles in solution. The monomer oxidation potentials ($1.75 < E^{ox} < 2.05$ vs SCE) were determined by cyclic voltammetry (CV) in solution of CH₂Cl₂ with 0.1 M of Bu₄NClO₄ and 0.005 M of monomer (Figure 1). Here, the difficulty is due to the presence of several oxidation peaks for these monomers due to the

several chemical parts (phenyl, thiophene, carbazole, naphthalene) but these peaks are above 1.75 V. Here, E^{ox} was chosen at the first intense peak.

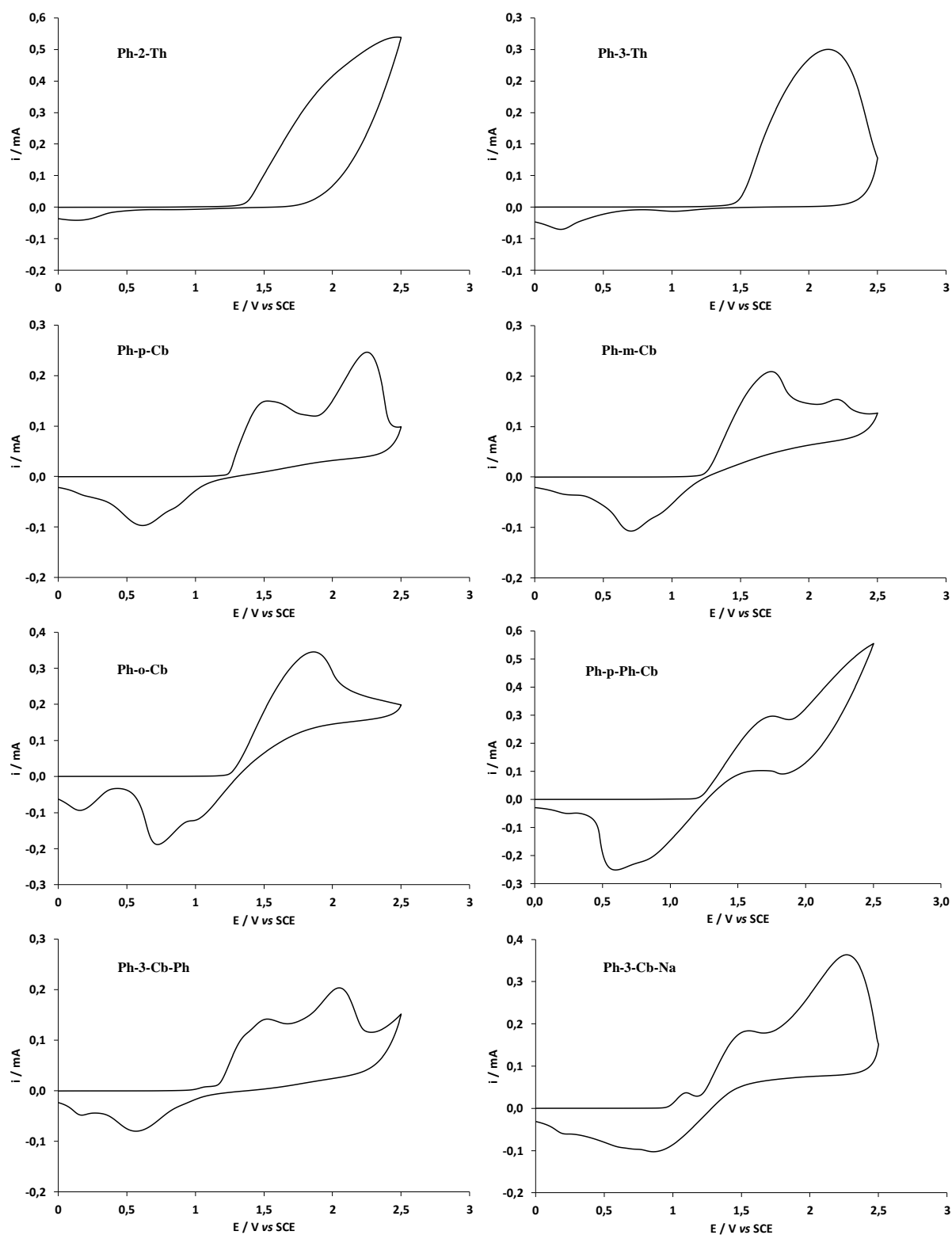


Figure 1. CV curves of each monomer. 1 scan from 0 V to 2.5 V with 0.1 M of Bu_4NClO_4 in CH_2Cl_2 . The scan rate was 100 mV s^{-1} .

Then, the electrodepositions were performed in the two solvents first by CV from -1 V to E^{ox} , a scan rate 20 mV s^{-1} and with different numbers of scans (1, 3 and 5). The depositions started from -1 V in order to produce H_2 bubbles in $\text{CH}_2\text{Cl}_2 + \text{H}_2\text{O sat.}$ ($2\text{H}^+ + 2\text{e}^- \rightarrow \text{H}_2$). The spectra are given in Figure 2. As expected, the peaks of water reduction are more intense in $\text{CH}_2\text{Cl}_2 + \text{H}_2\text{O sat.}$ However, the polymer oxidation and reduction peaks are particularly intense with **Ph-p-Ph-Cb**. This is surprising because carbazole gives only short oligomers compare to thiophene but the high intensity can be explained by a high deposition with this molecule and particularly by intermolecular π -stacking interactions.

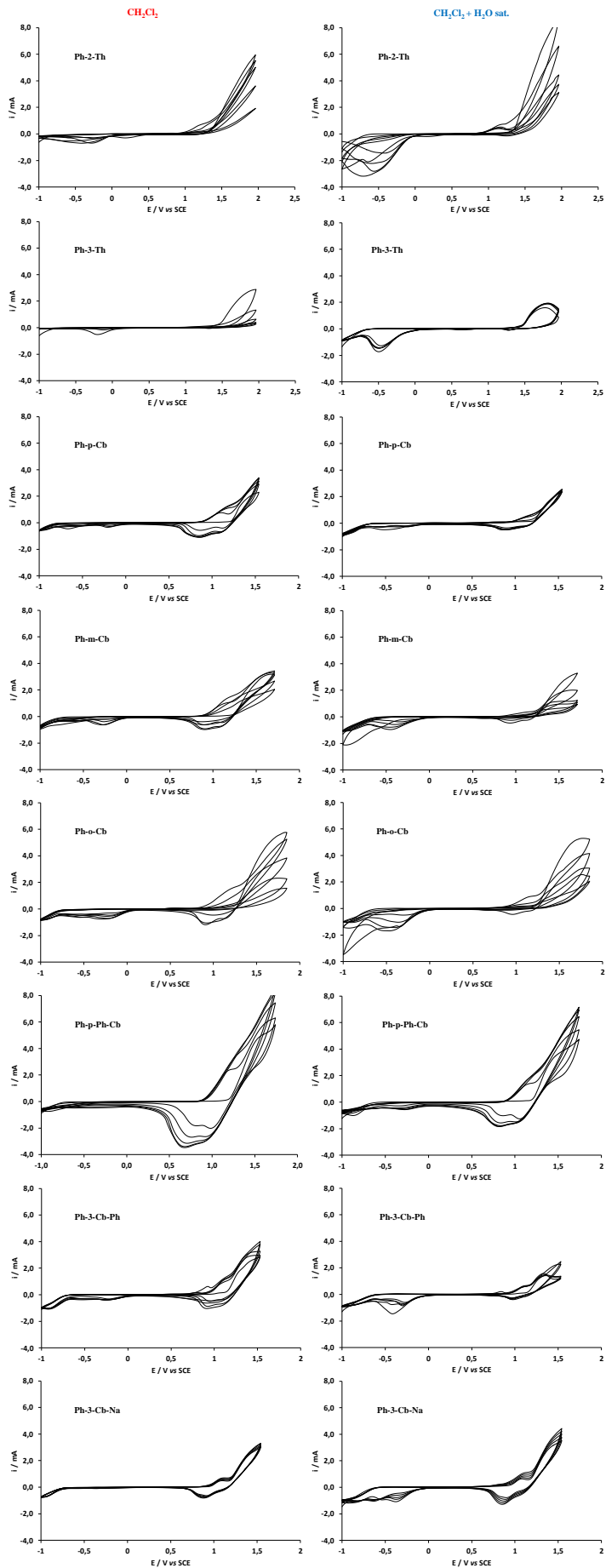


Figure 2. CV curves of each monomer. 5 scans from -1.0 V to E^{ox} V with 0.1 M of Bu_4NClO_4 in CH_2Cl_2 or $\text{CH}_2\text{Cl}_2 + \text{H}_2\text{O}$ sat. The scan rate was 20 mV s^{-1} .

After washing, the substrates were electrochemically characterized in solutions free of monomer. The CV curves of each polymer are available in Figure 3. First of all, this is the peak of the monomer which is the most intense in all CV curves indicating its majority presence in the electrodeposited films. This is surprising especially with thiophene moieties due to its high polymerization capacity compared to carbazole. Moreover, in the CV curves there is one peak for the monomer and another one for the oligomers with the thiophene-based monomers, and three peaks for the two for the carbazole-based monomers. For example, with **Ph-3-Cb-Ph** the peaks are relatively and well-separated, and are at 1.78, 2.02 and 2.22 V for the monomers and 0.92, 1.10 and 1.37 V for the oligomers.

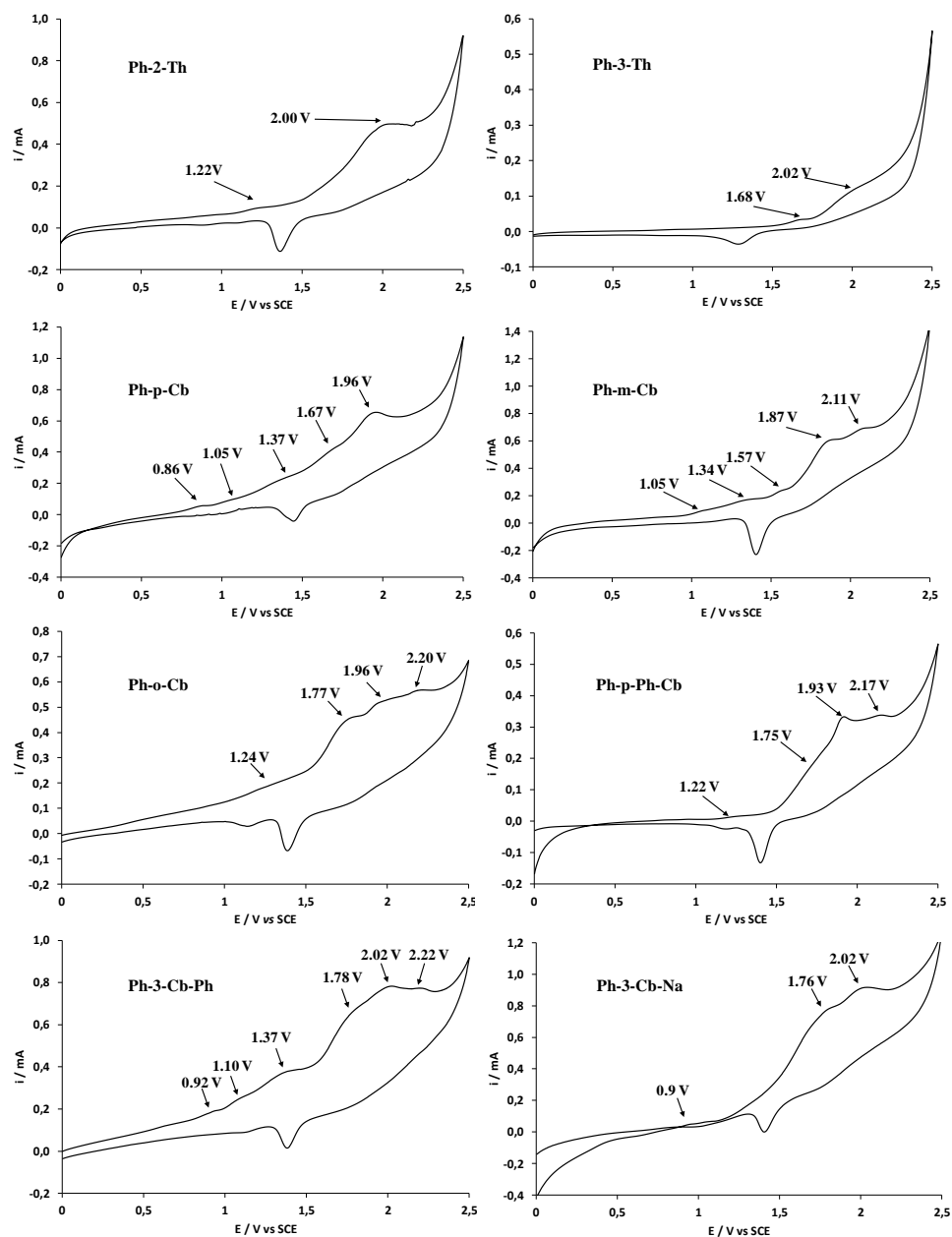


Figure 3. CV curves of electrodeposited surfaces from each monomer. 1 scan from 0 V to 2.5 V with 0.1 M of Bu_4NClO_4 in CH_2Cl_2 . The scan rate was 20 mV s^{-1} .

Electrodeposition by cyclic voltammetry

Scanning electron microscopy (SEM) images are available in Figure 4. First of all, both the monomer structure and H_2O content play key role in the final surface structures. In CH_2Cl_2 , the surfaces are either smooth or made of non-porous spherical particles. The formation of porous tubular structures is observed only with **Ph-m-Cb** but the number of structures on the surface is extremely low. The formation of porous structures by CV in CH_2Cl_2 can be expected by the formation of H^+ during electropolymerization ($n \cdot \text{Monomer} - 2n\text{e}^- \rightarrow \text{Polymer} +$

$2nH^+$), which after are reduced to H_2 bubbles during the back scans ($H_2 (2H^+ + 2e^- \rightarrow H_2)$ bubbles).

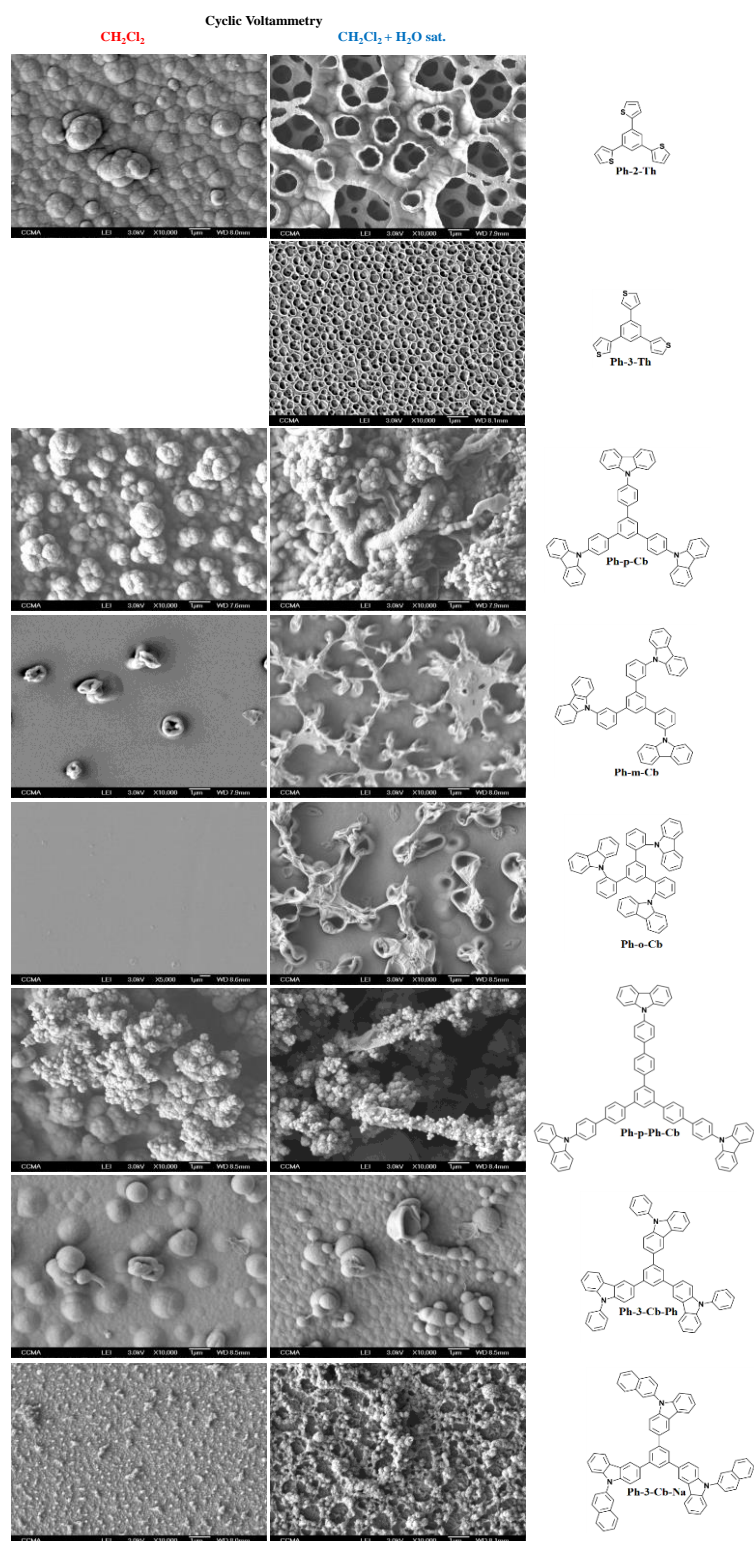


Figure 4. SEM images of electrodepositing surfaces from each monomer. 3 scans from -1 V to E^{ox} V with 0.1 M of Bu_4NClO_4 in CH_2Cl_2 or $CH_2Cl_2 + H_2O \text{ sat.}$ The scan rate was 20 mV s^{-1} .

In $\text{CH}_2\text{Cl}_2 + \text{H}_2\text{O}$ sat., the films made with the thiophene derivatives (**Ph-2-Th** and **Ph-3-Th**) are extremely porous resembling to corals. The size of the structures is extremely different ≈ 500 nm for **Ph-3-Th** and several μm for **Ph-2-Th**. Moreover, inside the huge structures of **Ph-2-Th** there are also clearly pores of lower size ($\approx 1 \mu\text{m}$) (Figure 5 and Figure 6). We already demonstrated that during electropolymerization in $\text{CH}_2\text{Cl}_2 + \text{H}_2\text{O}$ sat. there is the formation of inverse micelles^[27] and here the formation of these coral like-structures can be accepted by the presence of H_2O inside the micelles while during electropolymerization, the polymer grows around the bubbles due to the presence of CH_2Cl_2 and monomer but not inside the micelles. The size difference of the structures obtained with **Ph-2-Th** and **Ph-3-Th** can be also explained by the formation of micelles of smaller size with **Ph-3-Th**. Further analyses (Figure 5) show that the structures are formed after just 1 scan.

With carbazole-derivatives, it is observed sometimes the formation of tubules or ribbon-like structures that means there is a preferential growth in one or two directions with these monomers (Figure 4). This is the case with **Ph-m-Cb** and **Ph-o-Cb**. Further analyses with **Ph-m-Cb** (Figure 5) show that the ribbon-like structures are formed after just 3 scans. With carbazole at the *para*-position (**Ph-p-Cb**), this is both the formation of both long nanotubes and spherical particles, which can be explained by a higher insolubility in solution. This is confirmed also with **Ph-p-Ph-Cb**, for which the nanotubes become extremely long but with spherical particles.

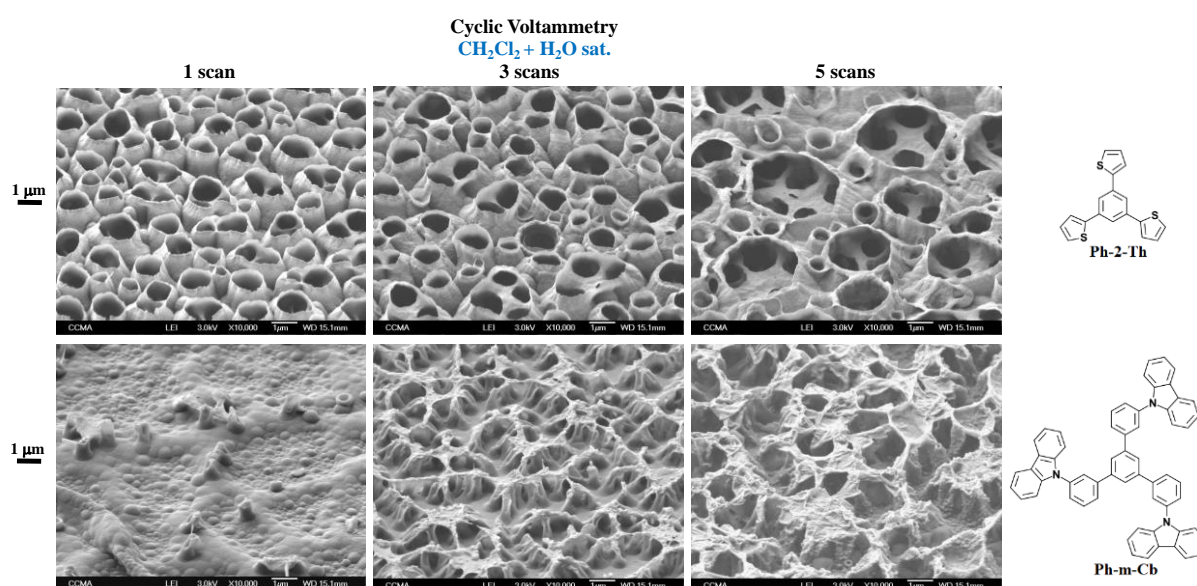


Figure 5. SEM images with an inclination angle of 45° of electrodeposited surfaces from **Ph-2-Th** and **Ph-m-Cb**. 1, 3 and 5 scans from -1 V to E^{ox} V with 0.1 M of Bu_4NClO_4 in $\text{CH}_2\text{Cl}_2 + \text{H}_2\text{O}$ sat. The scan rate was 20 mV s^{-1} .

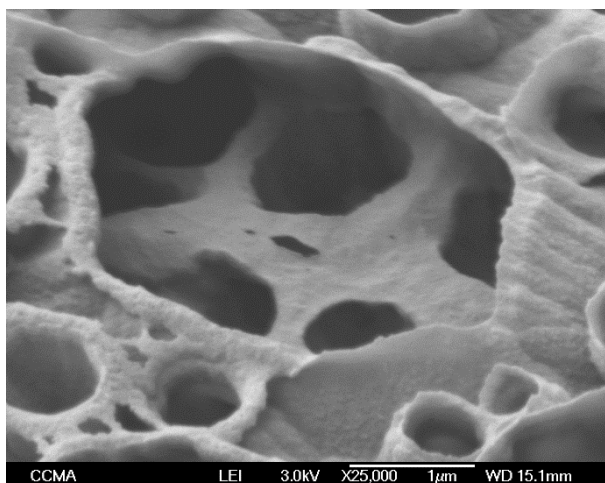


Figure 6. Supplementary SEM images with an inclination angle of 45° of electrodeposited surfaces from **Ph-2-Th**. 5 scans from -1 V to E^{ox} V with 0.1 M of Bu_4NClO_4 in $CH_2Cl_2 + H_2O$ sat. The scan rate was 20 mV s^{-1} .

The apparent contact angles (θ) were realized with probe liquids differing by their surface tension (γ_{LV}) (Table 1).

Table 1. Apparent contact angles for the rough and dedoped conducting polymer films prepared by cyclic voltammetry.

Monomer	Cyclic Voltammetry	Solvent: CH_2Cl_2			Solvent: $CH_2Cl_2 + H_2O$ sat.		
		θ_w ($^\circ$)	θ_{biiod} ($^\circ$)	θ_{Hexa} ($^\circ$)	θ_w ($^\circ$)	θ_{biiod} ($^\circ$)	θ_{Hexa} ($^\circ$)
Ph-2-Th	1	54.1	31.5	<10	63.3	<10	<10
	3	87.3	<10	<10	43.0	<10	<10
	5	63.8	<10	<10	71.9	<10	<10
Ph-3-Th	1	84.4	28.4	<10	58.8	28.5	<10
	3	78.9	13.1	<10	73.8	26.9	<10
	5	81.0	24.2	<10	86.6	<10	<10
Ph-p-Cb	1	85.5	<10	<10	70.8	<10	<10
	3	92.2	<10	<10	69.6	<10	<10
	5	91.0	<10	<10	87.4	<10	<10
Ph-m-Cb	1	85.6	40.6	<10	90.8	13.0	<10
	3	93.1	<10	<10	116.4	<10	<10
	5	97.9	<10	<10	135.9	19.7	<10
Ph-o-Cb	1	81.6	26.6	<10	70.0	<10	<10
	3	78.4	18.2	<10	119.0	<10	<10
	5	84.7	16.6	<10	133.0	<10	<10
Ph-p-Ph-Cb	1	141.3	<10	<10	147.0	<10	<10
	3	143.3	<10	<10	150.8	<10	<10
	5	132.9	<10	<10	105	<10	<10
Ph-3-Cb-Ph	1	99.3	26.1	<10	116.2	<10	<10
	3	106.0	<10	<10	122.6	<10	<10

	5	125.6	<10	<10	128.6	<10	<10
Ph-3-Cb-Na	1	118.8	25.4	<10	105.4	41.2	11.0
	3	85.5	14.9	<10	144.7	<10	13.9
	5	151.1	<10	<10	158.1	<10	<10

In order to better explain these results, smooth surfaces with each monomer were also prepared for determining the Young's angles (θ^Y)^[34] and the surface energy with the Owens-Wendt equation (Table 2).^[35] The films prepared with thiophene-based monomers (**Ph-2-Th**, **Ph-3-Th**) are intrinsically hydrophilic with $\theta_w^Y < 90^\circ$ while some of the films prepared with carbazole-based monomers (**Ph-p-Cb**, **Ph-m-Cb**, **Ph-3-Cb-Ph**) are intrinsically hydrophobic.

Table 2. Apparent contact angles and surface energy for the smooth and dedoped conducting polymer films.

Monomer	θ_w^Y (°)	θ_{Diiod}^Y (°)	θ_{Hexa}^Y (°)	γ_{SV}	$\gamma_{\text{SV,D}}$	$\gamma_{\text{SV,P}}$
Ph-2-Th	71.0	43.7	14.7	39.1	28.2	10.9
Ph-3-Th	77.6	54.0	16.9	34.3	26.2	8.1
Ph-p-Cb	97.2	47.7	13.0	31.0	30.2	0.8
Ph-m-Cb	94.1	56.6	19.5	28.8	27.0	1.8
Ph-o-Cb	83.5	55.5	18.1	31.8	26.5	5.3
Ph-p-Ph-Cb	89.8	48.8	16.2	31.5	28.9	2.6
Ph-3-Cb-Ph	96.6	58.1	17.5	28.3	27.1	1.2
Ph-3-Cb-Na	65.9	41.8	12.7	42.1	28.3	13.8

All the $\theta < \theta_w^Y$ when $\theta_w^Y < 90^\circ$, and reversely can be explained with the Wenzel equation (full wetting).^[36] All the $\theta > 90^\circ$ when $\theta_w^Y < 90^\circ$ can be explained only with the Cassie-Baxter equation indicating the presence of air between the droplet and the rough surface.^[37] Here, there is no relationship between the water apparent contact angles and the electrochemical parameters because, as shown by Cassie-Baxter, the main parameter affecting the apparent contact angles is the air fraction trapped between water droplet and the rough surface. Moreover, all the surfaces with high hydrophobicity, have also a sticking behavior comparable to rose petals or gecko foot.^[10–13] Indeed, water droplets remained stuck on the surface even with an inclination of 90° as shown in Figure 7. The advancing and receding contact angles and as a consequence the hysteresis can not be measured because water droplets do not move whatever the sliding angle.



Figure 7. Example of water droplet on our surfaces with an inclination angle of 90° .

Electrodeposition at constant potential

In order to confirm these results, another deposition method was tested with the same conditions: at constant potential ($E = E^{ox}$) and with different deposition charges. With this method, it is expected lower released gas bubbles because also oxygen O_2 bubbles can be formed from H_2O ($2H_2O - 4e^- \rightarrow O_2 + 4H^+$). This also possible in anhydrous CH_2Cl_2 if trace H_2O are present in solution. First of all, the surface structures (Figure 8) are very close to that obtained by CV confirming that the main parameters are the monomer structure and H_2O content. With **Ph-p-Ph-Cb**, extremely long tubes are also observed but especially at high deposition charge (400 mC cm^{-2}). Their surface hydrophobicity (θ_w) is a little lower (Table 3) which can be explained by the fact the conjugated polymers formed at imposed potentials are in their doped state and with hydrophilic perchlorate (ClO_4^-) anions. This doping has also an influence on the surface energy (γ_{LV}).

CH₂Cl₂

Imposed Potential

CH₂Cl₂ + H₂O sat.

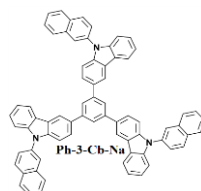
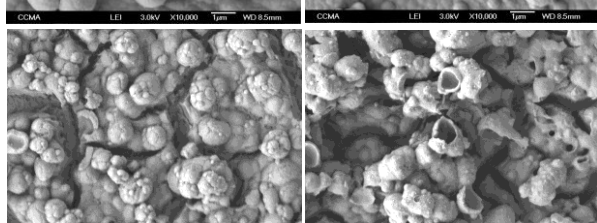
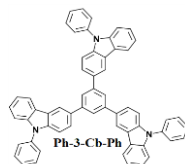
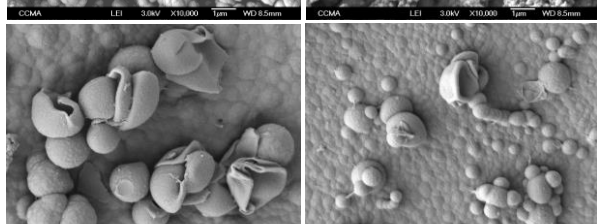
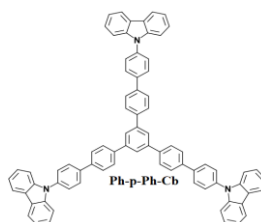
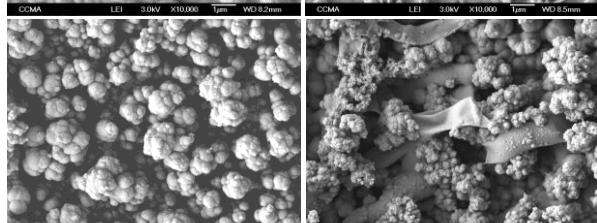
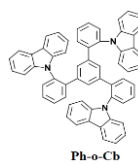
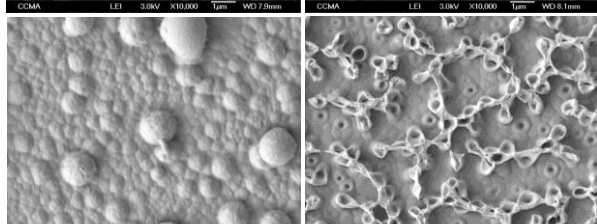
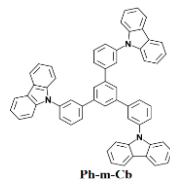
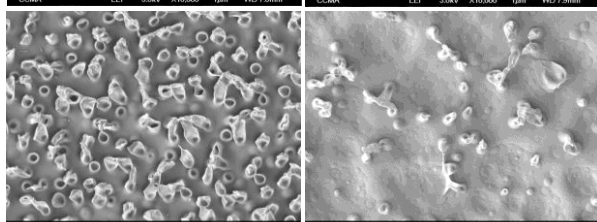
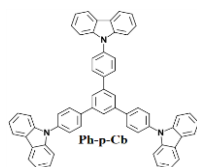
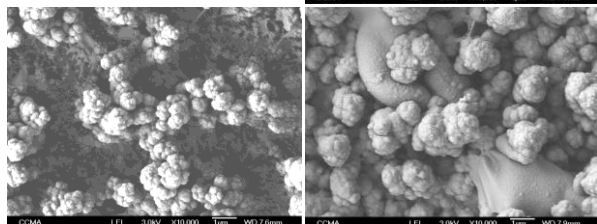
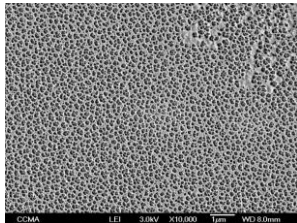
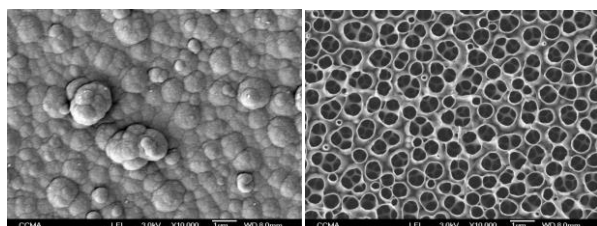


Figure 8. SEM images of electrodeposited surfaces from each monomer. At E^{ox} with 0.1 M of Bu_4NClO_4 in CH_2Cl_2 or $CH_2Cl_2 + H_2O$ sat. The deposition charge was 100 mC cm^{-2} .

Table 3. Apparent contact angles for the rough and doped conducting polymer films prepared at imposed potential.

Monomer	Imposed Potential	Solvent: CH_2Cl_2			Solvent: $CH_2Cl_2 + H_2O$ sat.		
		θ_w (°)	θ_{Diiod} (°)	θ_{Hexa} (°)	θ_w (°)	θ_{Diiod} (°)	θ_{Hexa} (°)
Ph-2-Th	12.5	75.4	20.4	<10	54.5	16.7	<10
	25	89.7	<10	<10	47.5	14.1	<10
	50	76.0	20.5	<10	32.3	22.1	<10
	100	64.0	<10	<10	33.5	28.6	<10
	200	68.1	<10	<10	40.3	42.5	<10
	400	68.3	<10	<10	<10	43.6	<10
Ph-3-Th	12.5	61.6	22.6	<10	51.8	34.6	<10
	25	64.7	26.7	<10	46.1	43.2	<10
	50	62.8	23.1	<10	54.2	47.1	<10
	100	84.1	<10	<10	35.9	51.8	<10
	200	85.2	25.2	<10	48.1	52.1	<10
	400	57.2	15.3	<10	<10	37.8	<10
Ph-p-Cb	12.5	75.4	<10	<10	71.7	<10	<10
	25	75.1	<10	<10	74.8	<10	<10
	50	74.5	<10	<10	76.0	<10	<10
	100	76.8	<10	<10	75.9	<10	<10
	200	68.7	<10	<10	69.6	<10	<10
	400	43.5	<10	<10	77.9	<10	<10
Ph-m-Cb	12.5	66.3	27.8	<10	64.6	32.6	<10
	25	60.9	32.9	<10	63.4	34.8	<10
	50	70.4	22.5	<10	67.6	34.3	<10
	100	50.6	16.3	<10	70.3	42.2	<10
	200	44.7	25.2	<10	64.8	27.9	<10
	400	45.4	31.0	<10	62.6	34.5	<10
Ph-o-Cb	12.5	65.5	23.7	<10	68.0	30.7	<10
	25	57.9	21.1	<10	61.0	31.1	<10
	50	58.3	27.5	<10	78.0	<10	<10
	100	50.7	22.1	<10	64.2	12.8	<10
	200	57.0	21.1	<10	71.1	23.4	<10
	400	59.1	23.0	<10	60.6	31.9	<10
Ph-p-Ph-Cb	12.5	101.6	24.0	<10	91.5	16.2	<10
	25	90.6	12.6	<10	95.4	<10	<10
	50	101.8	<10	<10	102.1	<10	<10
	100	105.1	<10	<10	102.6	<10	<10
	200	118.0	<10	<10	99.3	<10	<10
	400	113.1	<10	<10	95.8	<10	<10
Ph-3-Cb-Ph	12.5	74.2	14.4	<10	78.0	18.6	<10
	25	77.0	<10	<10	79.7	16.1	<10
	50	83.8	13.8	<10	76.5	14.4	<10
	100	92.5	22.1	<10	81.7	24.7	<10
	200	100.4	<10	<10	73.0	10.7	<10

	400	112.2	<10	<10	88.0	21.3	<10
Ph-3-Cb-Na	12.5	86.5	21.3	14.8	84.4	18.8	<10
	25	87.3	25.2	<10	88.6	24.2	<10
	50	79.4	<10	<10	84.7	21.8	<10
	100	84.6	<10	<10	80.8	<10	<10
	200	86.8	<10	<10	82.4	<10	<10
	400	110.7	<10	<10	61.5	<10	<10

Conclusion

To conclude, a soft-template electropolymerization was used by mixing H₂O is mixed to a solvent of low water-solubility (CH₂Cl₂) to form a micellar solution in the presence of Bu₄NClO₄ as electrolyte and surfactant. The monomers consisting in a benzene trifunctionalized with various thiophene and carbazole moieties were synthesized and used. As confirmed by cyclic voltammetry experiments, the monomers were fully conjugated to favor the deposition compared to polymerization. Tunable nanotubular structures (nanotubes, nano-ribbons, coral-like structures) were obtained and were dependent on the monomer and H₂O content but less on the deposition method. The maximum θ was 158.1° accompanied with strong water adhesive force comparable to gecko foot or rose petals. These surfaces could be used in the future in different applications such as in water-harvesting systems or in sensing platforms.

Supporting Information Summary

Supporting Information contains the monomer synthesis and experimental information.

Acknowledgements

The group thanks Christelle Boscagli from the Centre Commun de Microscopie Appliquée (CCMA, Université Côte d'Azur) for the preparation of the substrates necessary for the SEM analyses. This work was supported by CNRS GDR 2088 « BIOMIM ».

Received: ((will be filled in by the editorial staff))

Revised: ((will be filled in by the editorial staff))

Published online: ((will be filled in by the editorial staff))

Keywords: Conjugated polymers, Electropolymerization, Hydrophobicity, Nanotubes, Surface structures.

References

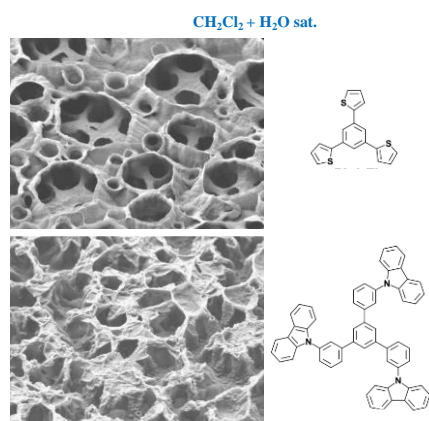
- [1] T. Y. Ren, Z. P. Miao, L. Ren, H. Xie, Q. Li, C. L. Xia, *Small* **2023**, *19*, 2205168.
- [2] G. T. Zan, Q. S. Wu, *Adv. Mater.* **2016**, *28*, 2099.
- [3] L. Y. Wen, Z. J. Wang, Y. Mi, R. Xu, S.-H. Yu, Y. Lei, *Small* **2015**, *11*, 3408.
- [4] S. H. Voon, L. V. Kiew, H. B. Lee, S. H. Lim, M. I. Noordin, A. Kamkaew, K. Burgess, L. Y. Chung, *Small* **2014**, *10*, 4993.
- [5] T. Darmanin, F. Guittard, *Mater. Today* **2015**, *18*, 273.
- [6] B. Su, Y. Tian, L. Jiang, *J. Am. Chem. Soc.* **2016**, *138*, 1727.
- [7] Y. Yang, Z. G. Guo, W. M. Liu, *Small* **2015**, *18*, 2204624.
- [8] Y. K. Lai, X. F. Gao, H. F. Zhuang, J. Y. Huang, C. J. Lin, L. Jiang, *Adv. Mater.* **2009**, *21*, 3799.
- [9] W. Barthlott, C. Neinhuis, *Planta* **1997**, *202*, 1.
- [10] C. R. Szczepanski, T. Darmanin, F. Guittard, *Adv. Colloid Interface Sci.* **2017**, *241*, 37.
- [11] L. Feng, Y. N. Zhang, J. M. Xi, Y. Zhu, N. Wang, F. Xia, L. Jiang, *Langmuir* **2008**, *24*, 4114.
- [12] B. Bhushan, M. Nosonovsky, *Phil. Trans. R. Soc. A* **2010**, *368*, 4713.
- [13] L. Qu, L. Dai, *Adv. Mater.* **2007**, *19*, 3844.
- [14] K. Wan, X. L. Gou, Z. G. Guo, *J. Bionic Eng.* **2021**, *18*, 501.
- [15] T. Kimura, M. Murase, Y. Yamada, N. Mizoshita, D. Nakamura, *Nanoscale Adv.* **2022**, *4*, 3718.
- [16] M. Marmur, *Langmuir* **2003**, *19*, 8343
- [17] C. Raufaste, G. Ramos Chagas, T. Darmanin, C. Claudet, F. Guittard, F. Celestini, *Phys. Rev. Lett.* **2017**, *119*, 108001.
- [18] Z. Cheng, J. Gao, L. Jiang, *Langmuir* **2010**, *26*, 8233.
- [19] K. K. S. Lau, J. Bico, K. B. K. Teo, M. Chhowalla, G. A. J. Amaratunga, W. I. Milne, G. H. McKinley, K. K. Gleason, *Nano Lett.* **2003**, *3*, 1701.
- [20] K. K. Jung, Y. Jung, C. J. Choi, J. S. Ko, *ACS Omega* **2018**, *3*, 12956.
- [21] H.-A. Lin, S.-C. Luo, B. Zhu, C. Chen, Y. Yamashita, H.-h. Yu, *Adv. Funct. Mater.* **2013**, *23*, 3212.
- [22] M. Pérez-Page, E. Yu, J. Li, M. Rahman, D. M. Dryden, R. Vidu, P. Stroeve, *Adv. Colloid Interface Sci.* **2016**, *234*, 51.
- [23] C. Debieuvre-Chouvy, A. Fakhry, F. Pillier, *Electrochim. Acta* **2018**, *268*, 66.

- [24] S. Gupta, *J. Raman Spectrosc.* **2008**, *39*, 1343.
- [25] J. T. Kim, S. K. Seol, J. H. Je, Y. Hwu, G. Margaritondo, *Appl. Phys. Lett.* **2009**, *94*, 034103.
- [26] L. Qu, G. Shi, F. Chen, J. Zhang, *Macromolecules* **2003**, *36*, 1063.
- [27] C. Fradin, F. Orange, S. Amigoni, C. R. Szczepanski, F. Guittard, T. Darmanin, *J. Colloid Interface Sci.* **2021**, *590*, 260
- [28] O. Thiam, A. Diouf, D. Diouf, S. Y. Dieng, F. Guittard, T. Darmanin, *Phil. Trans. R. Soc. A* **2019**, *377*, 20190123
- [29] M. Khodja, I. Bousrih, M. Kateb, M. Beji, F. Guittard, T. Darmanin, *J. Bionic Eng.* **2022**, *19*, 1054.
- [30] Y. C. Zhao, J. Stejskald, J. X. Wang, *Nanoscale* **2013**, *5*, 2620.
- [31] C. Fradin, F. Guittard, I. F. Perepichka, T. Darmanin, *Electrochim. Acta* **2022**, *425*, 140684.
- [32] S.-C. Luo, J. Sekine, B. Zhu, H. C. Zhao, A. Nakao, H.-h. Yu, *ACS Nano* **2012**, *6*, 3018.
- [33] S. L. Bai, Q. Hu, Q. Zeng, M. Wang, L. S. Wang, *ACS Appl. Mater. Interfaces* **2018**, *10*, 11319.
- [34] T. Young, *Phil. Trans. R. Soc. London* **1805**, *95*, 65.
- [35] D. K. Owens, R. C. Wendt, *J. Appl. Poly. Sci.* **1969**, *13*, 1741.
- [36] R. W. Wenzel, *Ind. Eng. Chem.* **1936**, *20*, 988.
- [37] A. B. D. Cassie, S. Baxter, *Trans. Faraday Soc.* **1944**, *40*, 546.

A soft-template electropolymerization is used with a solvent of low-water solubility in the presence of water to form a micellar solution. Monomers consisting in a benzene trifunctionalized various thiophene and carbazole moieties are investigated. The monomers are fully conjugated to favor the deposition compared to polymerization. Nanotubes are observed with some of the monomers indicating a preferential growth in one-direction.

P. D. Dione, Dr. A. Dramé, Prof. A. Diouf, Prof. F. Guittard, Dr. T. Darmanin*

Bioinspired Nanotubes by Soft-template Electropolymerization from Fully Conjugated Monomers



ToC figure ((Please choose one size: 55 mm broad \times 50 mm high **or** 110 mm broad \times 20 mm high. Please do not use any other dimensions))